Separation Science and Technology
Publication details, including instructions for authors and subscription information:
http://www.informaworld.com/smpp/title~content=t713708471

Separation of Binary Gas Mixture into Two High-Purity Products by a New Pressure Swing Adsorption Cycle

P. L. Cen[a]; R. T. Yang[a]
[a] Department of Chemical Engineering, State University of New York at Buffalo, Buffalo, New York

To cite this Article Cen, P. L. and Yang, R. T.(1986) 'Separation of Binary Gas Mixture into Two High-Purity Products by a New Pressure Swing Adsorption Cycle', Separation Science and Technology, 21: 9, 845 — 864
To link to this Article: DOI: 10.1080/01496398608058382
URL: http://dx.doi.org/10.1080/01496398608058382

SEPARATION SCIENCE AND TECHNOLOGY, 21(9), pp. 845-864, 1986

Separation of Binary Gas Mixture into Two High-Purity Products by a New Pressure Swing Adsorption Cycle

P. L. CEN and R. T. YANG*

DEPARTMENT OF CHEMICAL ENGINEERING
STATE UNIVERSITY OF NEW YORK AT BUFFALO
BUFFALO, NEW YORK 14260

Abstract

Binary mixtures can be separated into two high-purity products by a new pressure swing adsorption (PSA) cycle. The product purity depends on the purge/feed ratio of the respective gases in the PSA cycle. The process characteristics of the new PSA cycle, using activated carbon as the sorbent, can be adequately predicted by an equilibrium model.

INTRODUCTION

Since the invention of pressure swing adsorption (PSA) cycles in the late 1950s, namely Skarstrom and Guerin-Domine cycles, many sophisticated and efficient PSA cycles have been developed, and PSA has become an important separations tool in the chemical and petrochemical industries (*1, 2*).

In all commercial PSA cycles, the weakly adsorbed component in the mixture is the desired product. The strongly adsorbed component is usually of no value because of its low purity. This need not be the case if a PSA cycle is available by which a high-purity product for the strongly adsorbed component is obtained.

The bulk separation of binary mixtures using the commercial PSA cycles has been studied in this laboratory (*3*). Using activated carbon as the sorbent, the product purities of H_2 and CH_4 or CO are, respectively, 99+ and 90% at reasonably high product recoveries (*4, 5*). In order to

*To whom correspondence should be addressed.

 0149-6395/86/2109-0845$3.50/0

increase the purity of the strongly adsorbed component, i.e., CH_4 or CO, a new PSA must be used.

The product purity of the strongly adsorbed component is limited by the gas mixture occupying the void spaces in the bed. This product purity can be increased by displacing the gas mixture in the void spaces with a pure, strong adsorptive gas. For the separation of H_2/CH_4, the displacement can be accomplished by purging the bed with CH_4 after the adsorption step in the PSA cycle. This idea was first suggested in a patent by Tamura (*6*), which has been incorporated into the vacuum swing adsorption cycle for generating both N_2 and O_2 from air (*7*) and, on a pilot-plant scale, for generating N_2 from air by Torey Industries (*1*). No theoretical analysis or experimental data are available on this PSA cycle.

This paper reports a theoretical model and experiments for this PSA cycle for separating a 50/50 mixture of H_2/CH_4 using activated carbon. The experiments demonstrated that both H_2 and CH_4 products can be obtained at over 99% purity at high recoveries. The data can be adequately predicted by the equilibrium model. The important factors in the separation process are also studied both experimentally and theoretically.

The PSA Cycle

In the PSA cycle, each adsorber undergoes the following sequential steps, forming a complete cycle:

Step I: Repressurization
Step II: High-pressure adsorption
Step III: High-pressure purge by methane
Step IV: Countercurrent blowdown
Step V: Purge by hydrogen

Two or more interconnected adsorbers are operated synchronously so continuous feed and products are possible. The repressure step can be accomplished by either high-pressure H_2 product from another bed or the feed mixture. Pure H_2, however, was used in this study. The effects of repressure by H_2 or mixture have been studied in this laboratory (*5*). Steps I and V are conducted countercurrent to the feed direction to keep the H_2 product discharge end clean. Step III is in the cocurrent direction to keep the CH_4 discharge end free of H_2.

EXPERIMENTAL

A schematic of the apparatus is shown in Fig. 1. The one-column apparatus was designed to stimulate all steps in the PSA cycle and was capable of operating under a wide range of conditions. A detailed description of the apparatus is given in Ref. *3*. The characteristics of the adsorber column are given in Table 1.

The sorbent was PCB activated carbon, 20–60 mesh, manufactured by the Calgon Corporation. The H_2 gas was of the Extra Dry grade, supplied by the Linde Division. The H_2/CH_4 was premixed, also supplied by Linde. The CH_4 was also of Extra Dry grade from Linde.

A 10-min cycle was used in the experiments, with the following time distribution:

Step I: 0.5 min
Step II: 3.0 min
Step III: 3.0 min
Step IV: 2.5 min
Step V: 1.0 min

Each PSA run was initiated with a clean bed. The bed was cleaned by degassing at approximately 0.01 torr for 10 h. The run was continued until a cyclic steady state was reached. The concentration and flow rate of the

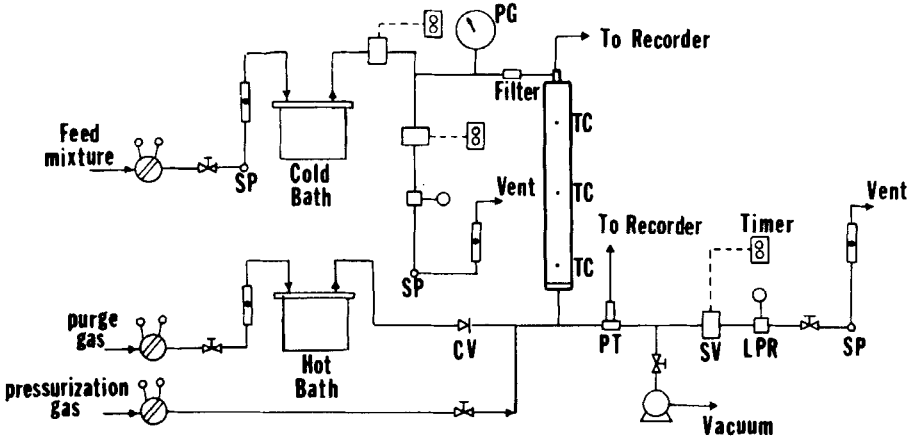

FIG. 1. Schematic diagram of apparatus for pressure swing adsorption for gas separation. SP: Sampling port. PG: Pressure gauge. CV: Check valve. PT: Pressure transducer. SV: Solenoid valve. TC: Thermocouple. LPR: Line pressure regulator.

TABLE 1
Adsorption Bed Characteristics

Bed inside radius, 2.05 cm
Bed length, 60 cm
Particle size, 0.028 cm
Bulk density, 0.498 g/cm^3
Particle density, 0.85 g/cm^3
Interparticle void fraction, 0.43
Intraparticle void fraction, 0.61
Total void fraction, 0.78
Heat capacity of carbon, 0.25 cal/g/°C

effluents, both H_2 and CH_4 products, were measured. A cyclic steady state was reached when these quantities no longer varied between cycles. The pressure history in the cycle was fixed and was recorded by a pressure transducer. The temperature histories were measured at three locations in the bed.

From the effluent composition and flow rate, the product purities and recoveries were calculated.

MATHEMATICAL MODEL

A number of models has been developed for bulk separation of multicomponent mixtures by PSA. These models are nonisothermal and include the mass transfer resistances at various accuracies (*3–5*). For binary PSA separations with activated carbon, the effects of mass transfer are not important, and the equilibrium model can adequately predict the separation results (*8*).

The equilibrium for the new PSA cycle is basically the same with other PSA models but differs in the boundary conditions. The cyclic process is initiated with a clean bed and is continued until a cyclic steady state is reached. The model predicts the concentration and flow rate of the effluent from the bed as functions of time. From these output data, results of separation can be calculated as product purities, product recoveries, and feed throughput.

The model equations are summarized below. The simplifying assumptions are: ideal gas behavior, negligible axial dispersion, negligible radial variations in temperature and concentration, local thermal equilibrium, and negligible mass transfer resistance.

The mass balance equations are

$$\frac{\partial uC}{\partial z} + \varepsilon \frac{\partial C}{\partial t} + \frac{\rho}{V_m} \frac{\partial q^*}{\partial t} = 0 \tag{1}$$

$$\frac{\partial uC_i}{\partial z} + \varepsilon \frac{\partial C_i}{\partial t} + \frac{\rho}{V_m} \frac{\partial q_i^*}{\partial t} = 0 \tag{2}$$

where $C_i = Py_i/RT$ and q_i^* is the equilibrium amount adsorbed. The energy balance equation is

$$\frac{\partial(uCC_pT)}{\partial z} + \varepsilon \frac{\partial(CC_pT)}{\partial t} \frac{\rho}{V_m} \frac{\partial[q(C_{pa}T - H)]}{\partial t} + \rho C_{ps} \frac{\partial T}{\partial t} + \frac{2h}{R}(T - T_0) = 0 \tag{3}$$

The last term in Eq. (3) represents the heat exchange between the bed and the surroundings.

The heat of adsorption, H, and heat capacities are calculated by

$$H = \sum X_i H_i \tag{4}$$

$$C_p = \sum y_i C_{pi} \tag{5}$$

$$C_{pa} = \sum X_i C_{pi} \tag{6}$$

$$C_{pi} = A_i + B_i T + C_i T^2 + D_i T^3 \tag{7}$$

where the summations are carried over all components.

The equilibrium mixture adsorption can be adequately calculated by the extended Langmuir isotherms or the loading ratio correlation. The data on H_2/CH_4 adsorption on activated carbon have been gathered in this laboratory (*9*). Thus,

$$q_i^* = q_{mi} \frac{B_i P_i^{n_i}}{1 + \sum_{j=1}^{N} B_j P_j^{n_j}} \tag{8}$$

where three constants are needed for pure-gas isotherms, and two of them are temperature dependent (Table 2):

$$q_{mi} = a_i + b_i/T$$

$$B_i = \exp(C_i + d_i/T)$$

TABLE 2
LRC Equation Coefficients:
Bi = exp $(C_i + d_i/T)$ (1/psi)
$q_{mi} = a_i + b_i/T$ (cm^3/g)

	a	b	c	d	n	H (cal/mol)
H_2	87.68	42392	−12.336	1219.3	0.97	2600
CH_4	−0.76	40539	−10.245	1756.0	1.00	5000

The initial conditions are taken at the end of bed pressurization (by hydrogen) in the first cycle. Thus,

$$y_{H_2} = X_{H_2} = 1.0$$
$$y_{CH_4} = X_{CH_4} = 0.0$$
$$P = P_f \qquad T = T_0, \qquad q = q_0$$

The boundary conditions for the ensuing cycles are:

Step II: Adsorption.

$$y_{H_2} = 0.5, \quad y_{CH_4} = 0.5, \quad P = P_f \quad T = T_f \quad u = u_f \quad \text{at } z = 0$$
$$P = P_f \quad \text{at } z = L$$

Step III: Cocurrent CH_4 Displacement

$$y_{H_2} = 0.0, \quad y_{CH_4} = 1.0, \quad P = P_f \quad T = T_f \quad u = u(t) \quad \text{at } z = 0$$
$$P = P_f \quad \text{at } z = L$$

Step IV: Countercurrent Blowdown

$$u = 0, \quad \text{at } z = L$$
$$P = P(t), \quad \text{at } t = t$$

Step V: Countercurrent H_2 Purge

$$y_{H_2} = 1.0, \quad y_{CH_4} = 0.0, \quad P = P_{\text{purge}}, \quad T = T_f \quad u = u_{\text{purge}}, \quad \text{at } z = L$$

Step I: H_2 Pressurization

$$u = 0, \quad \text{at } z = 0$$

$$y_{H_2} = 1.0, \quad y_{CH_4} = 0.0, \quad T = T_f \quad \text{at } z = L$$

$$P = P(t) \quad \text{at } t = t$$

The initial condition for Step II in the next cycle is the same as the final state of Step I, thus continuing the cyclic process.

The CH_4 feed rate, $u(t)$, is required as the boundary condition in Step III. It was, however, not measured in our experiments but could be calculated from the effluent flow rate by mass balance. The CH_4 feed rate was correlated by

$$u(t) = u_1 + u_2 t + u_3 t^2 \tag{9}$$

The constants u_1 to u_3 for all experiments are listed in Table 3.

The pressure history, $P(t)$, in Step IV was correlated by

$$P(t) = P_1 \exp(-P_2 t) \tag{10}$$

The pressure history curve was, however, unimportant in the new PSA cycle since the bed was filled with almost pure methane at the end of Step III. The parameters P_1 and P_2 are also listed in Table 3.

The overall heat transfer coefficient, h, in the heat balance equation was calculated *a priori* (*4*) as 9.58×10^{-5} cal/cm^2/K/s.

TABLE 3
The Coefficients for Eqs. (9) and (10):
$u = u_1 + u_2 t + u_3 t^2$ (mol/s)
$P = P_1 \exp(-P_2 t)$ (atm)

	Eq. (9) coefficients			Eq. (10) coefficients	
Run	$u_1 \times 10^3$	$u_2 \times 10^5$	$u_3 \times 10^7$	P_1	$P_2 \times 10^2$
1	7.6107	−3.569	−2.7778	14.61	1.0447
2	8.4722	−5.6977	0.8258	14.61	1.0447
3	7.5043	−2.8781	−0.4233	14.61	1.1391
5	10.3246	−8.1259	1.5933	21.4	1.7525
6	7.9568	−2.7203	−0.75563	21.4	1.7525
7	7.1796	−5.6397	1.6871	21.4	1.7525

Method of Solution

An implicit backward four-point finite difference method was used to solve Eqs. (1)-(8). The column was divided into 30 segments, and the time step was chosen to be 1.0 s. In this finite difference scheme, the composition and temperature of the effluent from each segment, in a given time interval, were the same as those in the segment, which resembled the tanks-in-series model in reactor design. A two-loop iteration scheme was developed to compute the composition, temperature, and flow rate of the effluent in each segment. The computation was initiated by assuming a set of values of C_i and T for that segment. Equation (8) was used to calculate q_i^*. The flow rate was then calculated by Eq. (1). From Eq. (2), C_i was calculated and compared with the assumed value. Iteration was continued until the calculated C_i was within 10^{-4} of the assumed value. Equation (3) was then used to calculate T, which was iterated until T was within 10^{-3} of the assumed value.

By using the above implicit difference scheme, the computation for the hyperbolic differential equations is unconditionally stable as discussed by Richtmyer and Morton (*10*).

All computations were performed in a VAX-780 computer. The cpu time was approximately 1.5 min. per PSA cycle. The cyclic steady state was reached after approximately 8 cycles in both experiments and model computation.

RESULTS AND DISCUSSION

The new PSA cycle was studied both experimentally and theoretically, i.e., by the equilibrium model which will be referred to as the EQ model. The independent process parameters were: H_2 purge/feed ratio, CH_4 purge/feed ratio, feed rate, pressure ratio (high P/low P in the cycle), as well as pressure history in the cycle. The effects of these parameters on the separation results were studied. These results, as well as an understanding of the bed dynamics during the cyclic process, are presented below.

Data Presentation for a Typical Run

The experimental data included: pressure history, temperature history at three locations in the column (namely, upper, middle, and lower points), instantaneous effluent composition and flow rate, and purge H_2

flow rate. All other parameters and variables must be calculated from these data by mass balance.

The feed rate or throughput was expressed as the feed amount (at STP) per cycle, which could be converted to sorbent productivity. The feed rate was calculated as follows. The mass balance was difficult to make because H_2 was contained in the feed in steps I, II, and IV, whereas CH_4 was in the feed in Steps II and III. The H_2 feed amount for bed repressurization (Step I) was estimated by assuming a clean bed in that step. This amount could then be calculated from the pressure increase and the H_2 adsorption isotherm. The estimate was within 5% of the model values which did not involve the clean bed assumption. The feed rate was then obtained as

$$\text{Feed/cycle} = \frac{(H_2 \text{ output in Steps II to V}) - (H_2 \text{ input in Steps I and V})}{\text{Mole fraction of } H_2 \text{ in feed}}$$

The amount of CH_4 used in Step III was then calculated by

$$CH_4 \text{ input in Step III} = (CH_4 \text{ output in Steps II to V}) - (CH_4 \text{ input in Step II})$$

The product recoveries were calculated as:

$$H_2 \text{ recovery} = \frac{(H_2 \text{ Output in Step II}) - (H_2 \text{ input in Steps I and V})}{H_2 \text{ input in Step II}}$$

$$CH_4 \text{ recovery} = \frac{(CH_4 \text{ output in Steps IV and V}) - (CH_4 \text{ input in Step III})}{(CH_4 \text{ input in Step II})}$$

The experimental results of a typical run, Run 1, are shown in Table 4 and Figure 2. From these data the separation results, in product purities and recoveries, were calculated and are given in Table 5. It is seen that both H_2 and CH_4 product were obtained at high purities. The recoveries and the throughput in the feed/cycle (459 L STP/hr/kg sorbent) were both within the ranges of commercial PSA operations. The EQ model results are also shown in Fig. 2 and Tables 4 and 5. A satisfactory agreement between model and experiment is seen.

TABLE 4
Steady-State PSA Process for Separating a 50/50 H_2CH_4 Gas Mixture. Experimental Data and Model Predictions for Run 1

Step	Time,[a] s	Effluent flow rate, L/min		Effluent composition (%)			
				H_2		CH_4	
		Expt	EQ	Expt	EQ	Expt	EQ
II	60	6.73	7.07	100.00	99.52	0.00	0.48
	120	6.60	7.08	97.35	98.58	2.65	1.42
	180	6.46	7.11	96.19	96.94	3.81	3.06
III	240	3.36	3.22	90.00	94.77	10.00	5.23
	270	2.75	2.74	78.13	91.15	21.89	8.85
	300	2.07	2.43	63.19	76.58	36.81	23.42
	330	1.76	2.36	26.07	51.19	73.93	48.81
	360	1.59	1.92	5.93	6.16	84.07	93.84
IV	420	12.18	10.78	0.11	0.04	99.89	99.96
	480	12.18	9.77	0.86	0.06	99.14	99.94
	510	10.63	9.25	0.63	0.08	99.37	99.92
V	555	5.23	6.91	2.08	1.11	97.92	98.89
	585	5.30	4.79	5.21	9.24	94.79	90.76

[a]Time begins from Step II.

Cyclic Dynamic Behavior of the Column

The dynamic bed behavior was well reflected by the temperature responses. The cyclic temperature histories are shown in Fig. 3. The EQ model predicted values compared favorably with the experimental data. The large temperature swing in the bed is characteristic of bulk PSA separation. A dip in temperature in the bed repressurization step was observed at the lower bed position, which was the inlet point for H_2 in this step. This dip was caused by desorption of CH_4. During the same step, a temperature rise was observed at the higher bed positions. The degree of temperature rise increased with the bed height. The rise was caused by the readsorption of CH_4. A stepped temperature rise was observed in the feed step, which corresponded to the CH_4 wavefront. The front was sharp due to the favorable isotherm of CH_4. During Step III, when pure CH_4

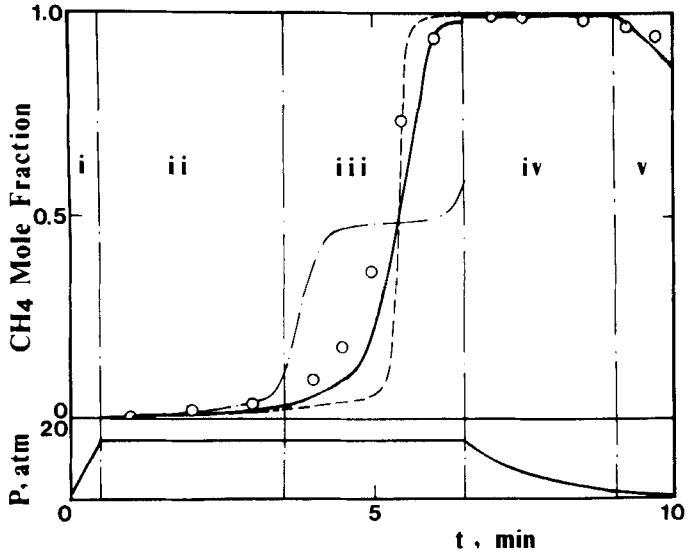

FIG. 2. Steady-state PSA cycle effluent concentration for separating a 50/50 H_2/CH_4 mixture for Run 1. Solid line: EQ model prediction. Circles: Experimental data. Case 1 (— · —) and Case 2 (- - -) are model predictions with cycle conditions shown in Table 7.

was fed in the bed, a second CH_4 wavefront propagated in the bed. The second or tailing front propagated at a higher velocity than the first, and in some runs caught up with the first one and merged into a single front, as will be shown shortly. The wavefront propagation velocity cannot be calculated with an analytic solution under the nonisothermal conditions. However, under isothermal condition and with constant interstitial flow velocity, v, the wavefront velocity, v_f, is given by

$$v_f = \frac{v}{1 + \dfrac{1 - \alpha}{\alpha} \dfrac{dq^*}{dC}} \tag{11}$$

The second term in the denominator dominates for CH_4 adsorption on carbon. This equation may be used to provide a qualitative understanding of the observed results. Since the interstitial velocity carrying the first front was higher than that carrying the second front, the faster-traveling second front was clearly due to a much lower value of dq^*/dC, the slope of

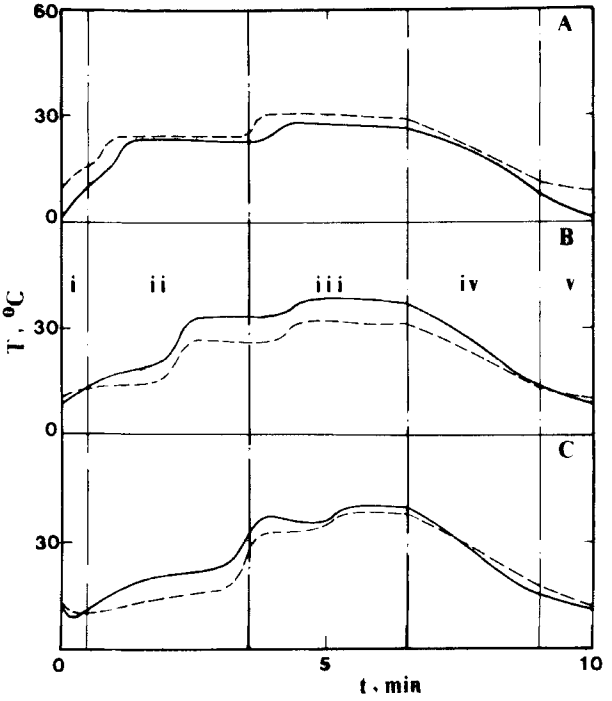

FIG. 3. Steady-state temperature histories in the PSA cycle at three bed locations: top (A), middle (B), and bottom (C), where the feed mixture enters from the top. Solid curves: Experimental. Dashed curves: Model predictions.

the isotherm. The slope of the isotherm indeed declined rapidly toward high concentrations, which was the case during CH_4 purge.

The gas-phase concentration profiles in the bed as simulated by the EQ model are shown in Fig. 4. The dynamic characteristics of the bed are clearly shown in the figure. The bed profile at $t = 0.5$ min corresponded to the end of the H_2 pressurization step, which showed the accumulation of CH_4 near the feed end of the adsorber as H_2 was introduced from the discharge end. The figure also shows the propagation of the two wavefronts, one for the 50/50 mixture feed and a tailing one for the CH_4 purge. The trailing wave eventually caught up with the leading one near the end of the bed, and merged into a single wave. At the end of the CH_4 purge step, $t = 6.5$ min, the bed was almost completely filled with CH_4.

TABLE 5

Steady-State PSA Separation of 50/50 H_2/CH_4 Mixture at a Feed Pressure of 14.61 atm. Pressure History Shown in Fig. 5. All Volumes in L STP

Run	1				2				3			
Feed gas, L/cycle	32.20				29.73				33.92			
Purge CH_4, L/cycle	16.61				17.08				17.97			
Purge H_2, L/cycle	0.79				0.81				0.76			
H_2 used in Step I, L/cycle	8.50				8.50				8.70			
End pressure of Step IV, atm	2.25				2.25				1.88			
	Output (L)		y_{CH_4}(%)		Output (L)		y_{CH_4}(%)		Output (L)		y_{CH_4}(%)	
Step	Expt	EQ	Expt	EQ	Expt	EQ	Expt	EQ	Expt	EQ	Expt	EQ
II	19.97	21.26	2.00	1.70	17.24	18.95	0.15	1.10	20.33	21.51	0.66	1.02
III	7.45	7.42	32.37	29.70	7.90	6.97	20.13	19.28	7.37	7.72	25.96	30.61
IV	25.91	24.84	99.49	99.95	25.58	24.67	99.06	99.95	28.75	26.29	99.65	99.95
V	5.27	5.55	96.30	95.14	5.39	6.04	91.56	94.58	4.70	6.00	93.72	94.17
H_2 recovery, %			61.93	68.40			48.98	62.35			63.30	68.10
CH_4 recovery, %			84.86	81.28			88.76	86.01			87.92	82.60

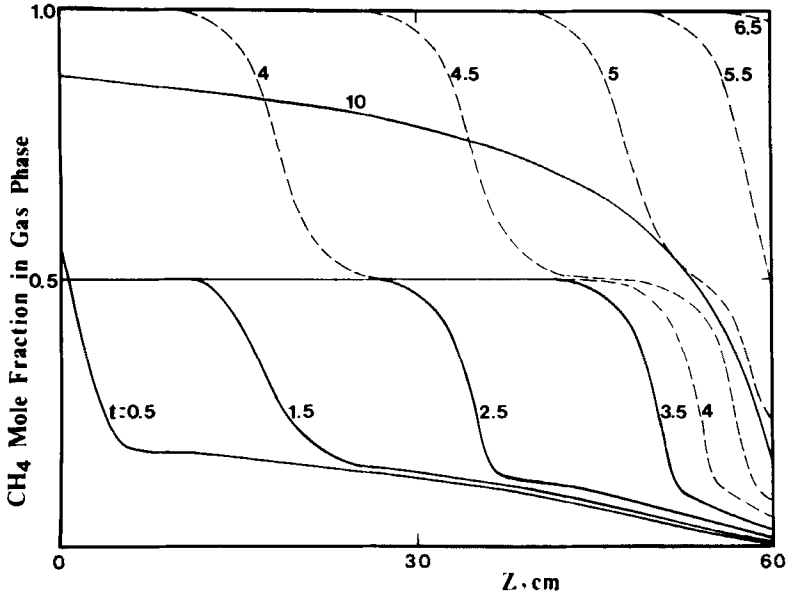

FIG. 4. Gas-phase composition in the bed in a steady-state PSA cycle at various times (in seconds) as marked.

Effects of Process Variables on Separation

The effects of process variables have been studied on the new PSA cycle. The variables were: H_2 purge/feed ratio, CH_4 purge/feed ratio, pressure ratio (which included the variations of both feed and H_2 purge pressures), and others. The ranges of variation for these variables were, however, not large since the cycles were carried out under nearly optimal conditions to yield a high purity for both products. Furthermore, it was not easy to change one variable at a time since some of the important variables, such as feed rate and CH_4 purge rate must be calculated by mass balance after the run as discussed in the foregoing. The results are summarized in Tables 5–7. The results for the three cases shown in Table 7 were predicted by the EQ model whereas for all other runs, both experimental and EQ model predictions are shown.

It has been well known that the purity of the light product (H_2) depends strongly on the purge/feed ratio by that light product (*8*). On the other hand, the purity of the heavy product (CH_4) will decrease as the H_2 purge/feed ratio is increased. This dependence was observed in the results given

TABLE 6

Steady-State PSA Separation of 50/50 H_2/CH_4 Mixture at a Feed Pressure of 21.4 atm. Pressure History Given in Fig. 5. All Volumes in L STP. Case 4 Gives Predicted Results by the Equilibrium Model Where Bed Repressurization Is by Step II Product, and Step III Is Preformed by the Product from Step IV after Compression

Run	5				6				7					
Feed gas, L/cycle	43.82				44.62				51.76					
Purge CH_4, L/cycle	19.08				18.97				15.83					
Purge H_2, L/cycle	1.16				0.80				0.90					
H_2 used in Step I, L/cycle	11.50				11.50				11.50					
End pressure of Step IV, atm	1.68				1.68				1.68					
	Output (L)		y_{CH_4}(%)		Output (L)		y_{CH_4}(%)		Output (L)			y_{CH_4}(%)		
Step	Expt	EQ	Expt	EQ	Expt	EQ	Expt	EQ	Expt	EQ	Case 4	Expt	EQ	Case 4
II	26.10	28.31	0.27	0.26	26.11	29.07	0.23	0.40	31.02	33.47	33.54	0.23	0.52	0.77
III	8.59	8.44	20.54	27.85	8.73	8.90	20.63	31.30	8.03	8.22	8.32	19.49	41.95	41.75
IV	33.49	31.63	99.22	99.94	33.65	32.18	99.33	99.96	35.64	31.78	31.69	99.41	99.56	99.21
V	7.38	7.33	87.20	89.55	6.41	6.31	93.52	92.52	4.82	6.53	6.53	89.42	91.46	91.44
H_2 recovery, %			61.02	70.03			61.59	71.80				76.11	80.53	79.35
CH_4 recovery, %			93.95	87.14			91.66	85.29				94.46	84.65	83.89

TABLE 7
Steady-State PSA Separation of 50/50 H_2/CH_4 Predicted by the EQ Model at a Fixed Total Amount of CH_4 Input in Steps II and III. In Case 3 the Bed Is Repressurized by Step II Product, and Step III is by Step IV Product

	Run 1				Case 1		Case 2		Case 3	
Feed gas, L/cycle					33.20		38.20		28.20	33.20
Purge CH_4, L/cycle					16.61		14.11		19.11	16.61
Purge H_2, L/cycle					0.79		0.79		0.79	0.79
Pressurization H_2, L/cycle					8.50		8.50		8.50	8.50
End pressure of Step IV, atm					2.25		2.25		2.25	2.25
	Output (L)		y_{CH_4} (%)							
Step	Expt	EQ	Expt	EQ	Output (L)	y_{CH_4} (%)	Output (L)	y_{CH_4} (%)	Output (L)	y_{CH_4} (%)
II	19.97	21.26	2.00	1.70	24.50	2.20	17.91	1.10	21.41	2.67
III	7.45	7.42	32.37	29.70	7.04	41.75	8.35	33.32	7.38	28.94
IV	25.91	24.84	99.43	99.95	24.40	98.96	24.48	99.96	24.83	99.84
V	5.27	5.55	96.30	95.14	5.48	94.35	5.57	94.91	5.54	95.13
H_2 recovery, %			61.93	68.40	76.85		60.24		67.11	
CH_4 recovery, %			84.86	81.28	79.62		75.52		81.04	

in Table 5. In Runs 1-3, shown in Table 5, the CH_4 purge/feed ratio as well as other variables were approximately fixed. A higher H_2 purge/feed yielded a higher H_2 product purity. Figure 5 shows $P(t)$ for all runs.

The effects of the CH_4 purge/feed ratio were similar to that of H_2, i.e., a higher CH_4 purge/feed ratio resulted in a higher CH_4 product purity. Also, the H_2 product purity declined as the CH_4 purge/feed ratio was increased due to the effects of dilution. This result is seen by comparing Runs 6 and 7, Table 6. In Table 3, the purge/feed ratios of both H_2 and CH_4 were changed in the three cases. The dilution effects were not as strong as the positive effects on the product purity as the purge/feed ratio was increased. Thus, both product purities were enhanced.

The ranges of conditions for Runs 1-3 were small. The same was true for Runs 5-7. However, the conditions were widely different between the two sets of runs. The results of separation were similar. Comparing Tables 5 and 6, it is clearly seen that, for the same separation, a higher throughput can be achieved by increasing the pressure ratio, i.e., feed pressure/H_2 purge pressure. In fact, they are approximately inversely proportional to each other.

In commercial systems, the purge gases are obtained from the process as portions of the effluents from other interconnected beds. In the experiments, pure gases were used. The effects on separation by using the process-derived gases were studied by the EQ model. The results are shown for Run 1 as Case 3 in Table 7 and for Run 7 as Case 4 in Table 6. It is seen from these results that almost identical separations were obtained whether pure gases or gases at purities as low as 97% were used for purge.

Comparison between Model and Experiment

Although the equilibrium model is capable of predicting all important characteristics of the PSA cycle, it showed a consistently higher H_2 recovery and a lower CH_4 recovery as compared with the experimental data. Possible causes for this discrepancy were: neglecting the pressure drop across the bed, inaccuracies in the model input parameters such as the $P(t)$ curve, and the equilibrium isotherms.

The $P(t)$ curve was measured at the H_2 discharge end. Therefore, the bed pressure was higher than the recorded value during Steps II and III, and lower during Steps IV and V. Consequently, more H_2 should have remained in the bed during Step II and more CH_4 should have been discharged during Steps IV and V, which resulted in the discrepancy.

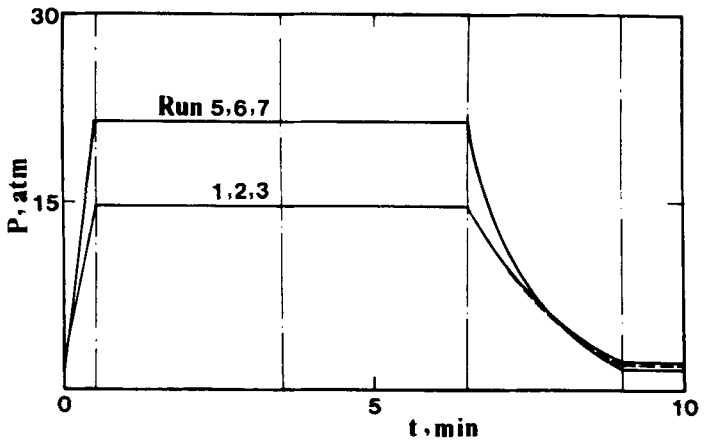

FIG. 5. Pressure histories for Runs 1-3 and 5-7.

CONCLUSIONS

1. The new PSA cycle is capable of separating a binary mixture into two high purity products. For example, a 50/50 H_2/CH_4 mixture can be separated by activated carbon into two products both at over 99% purity. The H_2 recovery is in the range 60-80% while the CH_4 recovery is nearly 90%. Compared to the commercial PSA cycles, additional energy is needed for the compression of the CH_4 product for the CH_4 purge step.

2. The H_2 product purity increases with the H_2 purge/feed ratio but decreases with the CH_4 purge/feed ratio. The CH_4 product purity increases with the CH_4 purge/feed ratio, but decreases with the H_2 purge/feed ratio. The cross adverse effects, however, are much weaker than the positive effects when a certain purge/feed ratio is increased.

3. The equilibrium model is adequate in predicting the PSA process characteristics with activated carbon as the sorbent.

SYMBOLS

A, B, C, D	the coefficients in the heat capacity equation
a, b, c, d	constants in adsorption isotherms
Bi	Langmuir constant (psi^{-1})
C	concentration in the gas phase ($mol/in.^3$)

C_p	gas heat capacity (cal/mol/K)
C_{pa}	heat capacity of the adsorbed phase (cal/mol/K)
C_{ps}	heat capacity of sorbent (cal/kg/K)
H	heat of adsorption (cal/mol)
h	overall heat transfer coefficient (cal/m^2/K/s)
L	total height of the column (m)
N	number of components
n	number of cells
n_i	loading-ratio correlation constants
P	total pressure (atm)
q	adsorbed amount (m^3 STP/kg)
q_m	Langmuir constant (m^3 STP/kg)
R	radius of column (m)
T	temperature (K)
t	time (s)
u	superficial flow rate (m/s)
V_m	molar volume at STP (m^3/mol)
x	mole fraction in adsorbed phase
y	mole fraction in gas phase
z	axial distance in the column (= 0 at the feed end) (m)

Greek Symbols

ε	interparticle void fraction
ρ	bed density (kg/m^3)

Superscripts

*	equilibrium

Subscripts

f	feed, fluid phase
i	component i

Acknowledgment

This work was supported by the U.S. Department of Energy under Grant No. DE-AC21-83MC20183.

REFERENCES

1. R. T. Yang, *Gas Separation by Adsorption Processes,* Butterworths, Stoneham, Massachusetts, 1986, Chaps. 7 and 8.
2. (a) G. E. Keller, *Industrial Gas Separations* (T. E. Whyte et al., eds.), American Chemical Society, Washington, D.C., 1983, p. 145. (b) R. T. Cassidy and E. S. Holmes, *AIChE Symp. Ser., No. 233 (Vol. 80),* 68 (1984).
3. R. T. Yang, S. J. Doong, and P. L. Cen, *AIChE Symp. Ser., No. 242 (Vol. 81),* 84 (1985).
4. P. L. Cen and R. T. Yang, *Ind. Eng. Chem., Fundam.,* In Press.
5. R. T. Yang and S. J. Doong, *AIChE J., 31,* 1829 (1985).
6. T. Tamura, U.S. Patent 3,797,201 (1974).
7. S. Sircar and J. W. Zondlo, U.S. Patent 4,013,429 (1977).
8. S. J. Doong and R. T. Yang, *Chem. Eng. Commun., 41,* 163 (1986).
9. J. T. Saunders and R. T. Yang, *Fuel, 64,* 621 (1985).
10. R. D. Richtmyer and K. W. Morton, *Difference Methods for Initial-Value Problems,* 2nd ed., Wiley-Interscience, New York, 1967, p. 233.

Received by editor October 7, 1985